# Adaptive evolution in virulence effectors of the rice blast fungus *Pyricularia oryzae*

Le Naour--Vernet Marie[1*], Charriat Florian[1*], Gracy Jérôme[2], Cros-Arteil Sandrine[1], Ravel Sébastien[1,3], Veillet Florian[1], Meusnier Isabelle[1], Padilla André[2], Kroj Thomas[1], Cesari Stella[1**], Gladieux Pierre[1**]

[1]PHIM Plant Health Institute, Univ Montpellier, INRAE, CIRAD, Institut Agro, IRD, Montpellier, France

[2]Centre de Biologie Structurale (CBS), Univ Montpellier, INSERM, CNRS, 29 rue de Navacelles, 34090 Montpellier, France.

[3]CIRAD, UMR PHIM, 34090 Montpellier, France

* These authors contributed equally to this work

** Corresponding authors:

Pierre Gladieux

Tel: +33 4 99 62 48 17

Email: pierre.gladieux@inrae.fr

Stella Cesari

Tel: +33 4 99 62 48 62

Email: stella.cesari@inrae.fr

Short title: MAX effector evolution in the rice blast fungus

## ABSTRACT

Plant pathogens secrete proteins called effectors that target host cellular processes to promote disease. Recently, structural genomics has identified several families of fungal effectors that share a similar three-dimensional structure despite remarkably variable amino-acid sequences and surface properties. To explore the selective forces that underlie the sequence variability of structurally-analogous effectors, we focused on MAX effectors, a structural family of effectors that are major determinants of virulence in the rice blast fungus *Pyricularia oryzae*. Using structure-informed gene annotation, we identified 58 to 78 MAX effector genes per genome in a set of 120 isolates representing seven host-associated lineages. The expression of MAX effector genes was primarily restricted to the early biotrophic phase of infection and strongly influenced by the host plant. Pangenome analyses of MAX effectors demonstrated extensive presence/absence polymorphism and identified gene loss events possibly involved in host range adaptation. However, gene knock-in experiments did not reveal a strong effect on virulence phenotypes suggesting that other evolutionary mechanisms are the main drivers of MAX effector losses. MAX effectors displayed high levels of standing variation and high rates of non-synonymous substitutions, pointing to widespread positive selection shaping the molecular diversity of MAX effectors. The combination of these analyses with structural data revealed that positive selection acts mostly on residues located in particular structural elements and at specific positions. Our work provides unique insights into the evolutionary history of an extended fungal effector family and opens up new research avenues to deepen our understanding of the molecular coevolutionary interactions of fungi with plant hosts.

## AUTHOR SUMMARY

Fungal plant pathogens use small secreted proteins, called effectors, to manipulate to their own advantage their host's physiology and immunity. The evolution of these effectors, whether spontaneously or in response to human actions, can lead to epidemics or the emergence of new diseases. It is therefore crucial to understand the mechanisms underlying this evolution. In this article, we report on the evolution of effectors in one of the prime experimental model systems of plant pathology, the fungus causing blast diseases in rice, wheat, and other cereals or grasses. We identify a particular class of effectors, the MAX effectors, using structural models based on experimental protein structures of effectors previously shown to have a major role in fungal virulence. We show that this class of effector is produced by the pathogen during the early stages of infection, when plant cells are still alive. By comparing the gene content of isolates infecting different plant species, we show that the MAX effector arsenal is highly variable from one isolate to another. Finally, using the inferential framework of population genetics, we demonstrate that MAX effectors exhibit very high genetic variability and that this results from the action of natural selection.

## INTRODUCTION

Plant pathogens secrete effector proteins to manipulate the physiology and metabolism of their host and to suppress its immunity. Consequently, effectors are expected to engage in coevolutionary interactions with plant defense molecules. The proximate mechanisms of effector-driven adaptation are relatively well-characterized: plant pathogens adapt to new hosts through changes in effector repertoires and effector sequences [1, 2]. However, the ultimate (eco-evolutionary) mechanisms underlying effector diversification have remained elusive. The concept of coevolution posits that adaptation in one partner drives counter-adaptations in the coevolving partner [3-5]. Under the co-evolutionary arms race model, variation for disease resistance and pathogen virulence is transient, resulting in a turnover of sequence variation through repeated episodes of strong directional selection [6]. In agricultural systems, because pathogens tend to be ahead of their hosts in the arms race owing to their larger populations and shorter generation times, the co-evolutionary arms race tends to result in so-called boom and bust cycles [7]. Under the alternative, 'trench warfare' hypothesis, advances and retreats of resistance or virulence genes frequencies maintain variation as dynamic polymorphisms [8, 9]. The maintenance of genetic polymorphisms is called 'balancing selection', a process by which different alleles or haplotypes are favored in different places (via population subdivision) and/or different times (via frequency-dependent negative selection). While there is a growing body of data demonstrating the nature and prevalence of the selective pressures that shape the diversity of immune systems in plants [6, 10-12], we still lack a clear picture of the co-evolutionary mechanisms underlying the molecular evolution of virulence factors in their interacting antagonists [13].

Effectors from plant pathogenic fungi are typically cysteine-rich secreted proteins smaller than 200 amino acids with an infection-specific expression pattern. Effectors are numerous in fungal genomes (several hundred to more than a thousand per genome), and rarely show homologies with known proteins or domains. They are also highly variable in sequence and do not form large families of sequence homologs. Based on similarity analyses, fungal effectors can form small groups of paralogs (typically with less than five members), but they are most often singletons. This apparent lack of larger effector families has hindered attempts to probe into the evolutionary factors underlying their diversification. In addition, the high diversity of fungal effectors has hampered functional analyses due to the lack of good

criteria for prioritizing them and our inability to predict their physiological role. Consequently, the virulence function and evolutionary history of most fungal effectors remain unknown.

Recently, the resolution of the three-dimensional (3D) structure of fungal effectors combined with Hidden Markov Model (HMM) pattern searches and structure modeling revealed that fungal effector repertoires are, despite their hyper-variability, dominated by a limited number of families gathering highly sequence-diverse proteins with shared structures and, presumably, common ancestry [14-17]. One such structurally-conserved but sequence-diverse fungal effector family is the MAX (*Magnaporthe* Avrs and ToxB-like) effector family. MAX effectors are specific to ascomycete fungi and show massive expansion in *Pyricularia oryzae* (synonym: *Magnaporthe oryzae*) [17], the fungus causing rice blast disease, one of the most damaging diseases of rice [18, 19]. MAX effectors are characterized by a conserved structure composed of six β-strands organized into two antiparallel β-sheets that are stabilized in most cases by one or two disulfide bridges. The amino acid sequence of MAX effectors is very diverse and they generally have less than 15% identity, which makes them a family of analogous, not homologous effectors. MAX effectors are massively expressed during the biotrophic phase of infection, suggesting an important role in disease development and fungal virulence [17]. Remarkably, about 50% of the known avirulence (AVR) effectors of *P. oryzae* belong to the MAX family, indicating that these effectors are closely monitored by the host plant immune system [17].

*Pyricularia oryzae* is a multi-host, poly-specialist pathogen that infects more than 50 monocotyledonous plants, including major cereal crops such as rice, maize, wheat, or barley [20-23]. *Pyricularia oryzae* has repeatedly emerged on new hosts [21, 24], in new geographical areas [25, 26], and phylogenomic analyses have revealed that it can be subdivided into several genetic lineages, each preferentially associated with a specific or restricted set of host plant genera [27]. In *P. oryzae*, effectors can play a major role in host-shifts or host-range expansions [28-30]. For example, loss of function of the PWT3 effector in *Lolium*-infecting strains contributed to gain of virulence on wheat [29]. Similarly, loss of the MAX effector AVR1-CO39 is thought to have contributed to the emergence of rice blast from foxtail-millet infecting isolates [20, 31]. This indicates that MAX effectors may be important determinants of host specificity in *P. oryzae*.

In this study, we characterized the genetic diversity of MAX effectors in *P. oryzae* and within its different host-specific lineages. We explored the evolutionary drivers of the diversification of MAX effectors and tested whether MAX effectors represent important determinants of *P. oryzae* host specificity. To this aim, we assembled and annotated 120 high-quality *P. oryzae* genomes from isolates representing seven main host-specific lineages. We mined these genomes for putative effectors and used hidden Markov models based on fold-informed protein alignments to annotate putative MAX effectors. We identified 58 to 78 putative MAX effector genes per individual genome distributed in 80 different groups of MAX homologs. We showed that the expression of *MAX* effector genes is largely restricted to the early biotrophic phase of infection and strongly influenced by the host plant. Our evolutionary analyses showed that MAX effectors harbor more standing genetic variation than other secreted proteins and non-effector genes, and high rates of non-synonymous substitutions, pointing to positive selection as a potent evolutionary force shaping their sequence diversity. Pangenome analyses of MAX effectors demonstrated extensive presence/absence polymorphism and identified several candidate gene loss events possibly involved in host range adaptation. Our work demonstrates that MAX effectors represent a highly dynamic compartment of the genome of *P. oryzae*, likely reflecting intense co-evolutionary interactions with host molecules.

## RESULTS

*Genome assembly and prediction of MAX effector genes.*

We assembled the genomes of a worldwide collection of 120 haploid isolates of *Pyricularia oryzae* fungi from 14 host genera: *Oryza* (n=52), *Triticum* (n=21), *Lolium* (n=12), *Setaria* (n=8), *Eleusine* (n=8), *Echinochloa* (n=4), *Zea* (n=4), *Bromus* (n=2), *Brachiaria* (n=2), *Festuca* (n=2), *Stenotaphrum* (n=2), *Eragrostis* (n=1), *Hordeum* (n=1), and *Avena* (n=1) (S1 Table). Assembly size ranged from 37Mb to 43.2Mb, with an average size of 40.2 Mb (standard deviation [s.d.]: 1.9Mb). L50 ranged from five to 411 contigs (mean: 97.1; s.d.: 83.2) and N50 from 28Kb to 4.0Mb (mean: 238.6Kb; s.d.: 43.8Kb; S1 Table). Gene prediction based on protein sequences from reference 70-15 and RNAseq data identified 11,520 to 12,055 genes per isolate (mean: 11,763.2; s.d.: 103.7). The completeness of assemblies, as estimated using BUSCO [32], ranged between 93.4 and 97.0% (mean: 96.4%; s.d.: 0.6%; S1 Table).

MAX effectors were identified among predicted secreted proteins using a combination of similarity searches [33, 34] and structure-guided alignments [35] as summarized in Figure 1. To assess variation in the MAX effector content of *P. oryzae*, we constructed groups of homologous genes (i.e., "orthogroups" or OG) using the clustering algorithm implemented in ORTHOFINDER [36]. A given orthogroup was classified as secreted proteins or MAX effectors if 10% of sequences in the group were identified as such by functional annotation. Sequences were grouped in 14,767 orthogroups, of which 80 were classified as encoding MAX effectors, and 3,283 as encoding other types of secreted proteins (Figure 1). The number of MAX orthogroups per isolate ranged from 58 to 73 (average: 65.8; s.d.: 2.8), representing between 58 to 78 *MAX* genes per isolate (average: 68.4; s.d.: 3.6). The 80 orthogroups of MAX effectors were further split into 94 groups of orthologs, by identifying paralogs using gene genealogies inferred with RAXML v8 [37] (S2 Table).

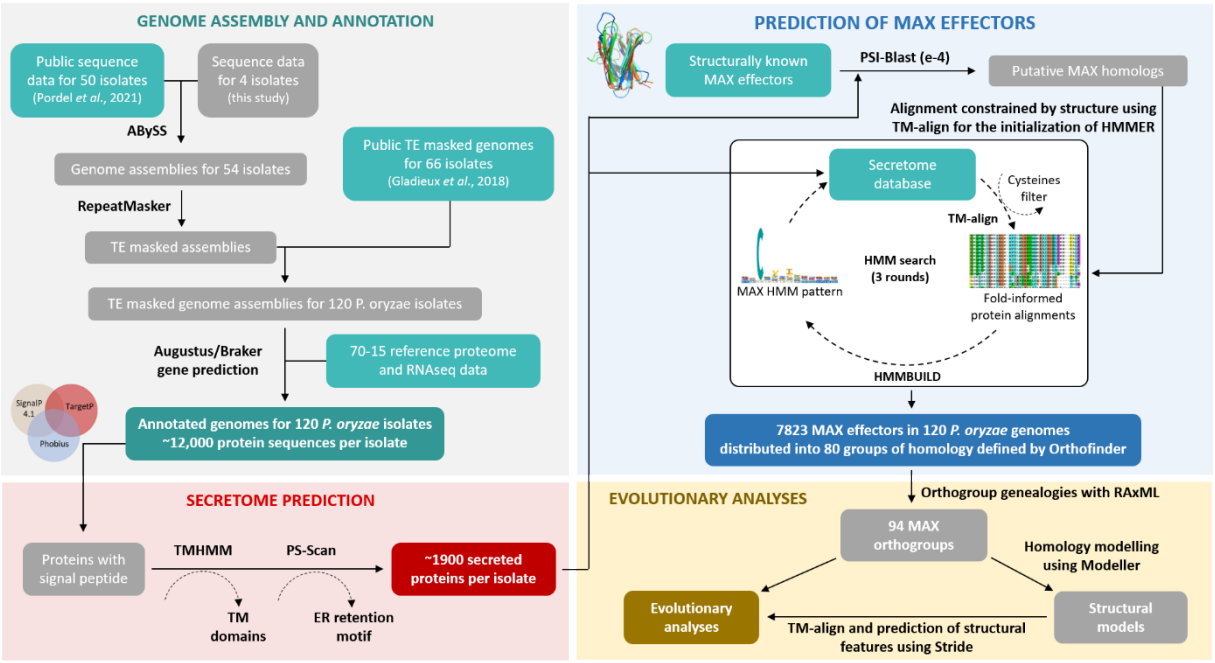


Figure 1. Schematic representation of the key steps of the bioinformatic pipeline used to predict genes in 120 genomes of *Pyricularia oryzae*, and to identify genes encoding MAX effectors. References: Gladieux et al. 2018 [27]; Pordel et al. 2021 [21].

*Expression of MAX effector genes during rice infection.*

To determine whether these putative MAX effectors are deployed by *P. oryzae* during plant infection, we analyzed the expression patterns of the 67 *MAX* genes predicted in the genome of the reference isolate Guy11 by qRT-PCR (Figure 2A). Using RNA samples from Guy11 mycelium grown on artificial media, we found that 94% of the *MAX* genes (63 genes) were not, or very weakly expressed during axenic culture, and only four (i.e., *MAX24*, *MAX29, MAX59,* and *MAX66*) showed weak, medium or strong constitutive expression (Figure 2A). *MAX* genes were, therefore, predominantly repressed in the mycelium of *P. oryzae*.

Following spray inoculation of Guy11 on the rice cultivar Maratelli, which is highly susceptible to *P. oryzae*, 67% of the *MAX* genes (45 genes) were expressed (Figure 2A). Among them, three were also expressed in the mycelium (i.e., *MAX31, MAX59*, and *MAX94*). *MAX31* was over-expressed under infection conditions, whereas the other two showed similar levels of expression *in vitro* and during infection. 64% of the *MAX* genes (42 genes) showed an infection-specific expression profile with relative expression levels ranging from very low (0.008-0.04) to very high (>5). Like the *Bas3* gene, encoding a *P.*

175 *oryzae* effector specifically induced during the biotrophic phase of infection, all *MAX* genes showed
176 maximal expression between the second and fourth day post-inoculation (Figure 2A; S1 Figure).
177 To test whether the genotype of the host plant could influence the expression of *MAX* genes, we
178 analyzed their expression patterns upon infection of the rice cultivar Kitaake, which has a higher basal
179 resistance to *P. oryzae* than Maratelli (Figure 2A; Figure 2B). During Kitaake infection, 78% of the *MAX*
180 genes (52 genes) were upregulated compared to the *in vitro* condition, while only 64% (43 genes) were
181 induced upon infection of Maratelli (Figure 2A). Some *MAX* genes not expressed in Maratelli were
182 induced in Kitaake (e.g., *MAX24, MAX30, MAX32, MAX43, MAX71,* and *MAX73*) (Figure 2B, S2 Figure).
183 Others were significantly upregulated in Kitaake compared to Maratelli (i.e., *MAX22, MAX44, MAX55,*
184 *MAX57, MAX69*, and *MAX91*). However, a few genes, such as *MAX15, MAX37* and *MAX62*, among the
185 most strongly expressed effectors in Maratelli, showed weaker levels of expression in Kitaake. These
186 results show that Guy11 deploys a wider diversity of MAX effectors during the infection of Kitaake
187 compared to that of Maratelli, and that MAX effectors are subject to host-dependent expression
188 polymorphism.
189 Taken together, our data revealed that during the biotrophic phase of rice infection, *P. oryzae*
190 massively deploys MAX effectors in a plastic manner suggesting that they have an important function in
191 fungal virulence.
192
193

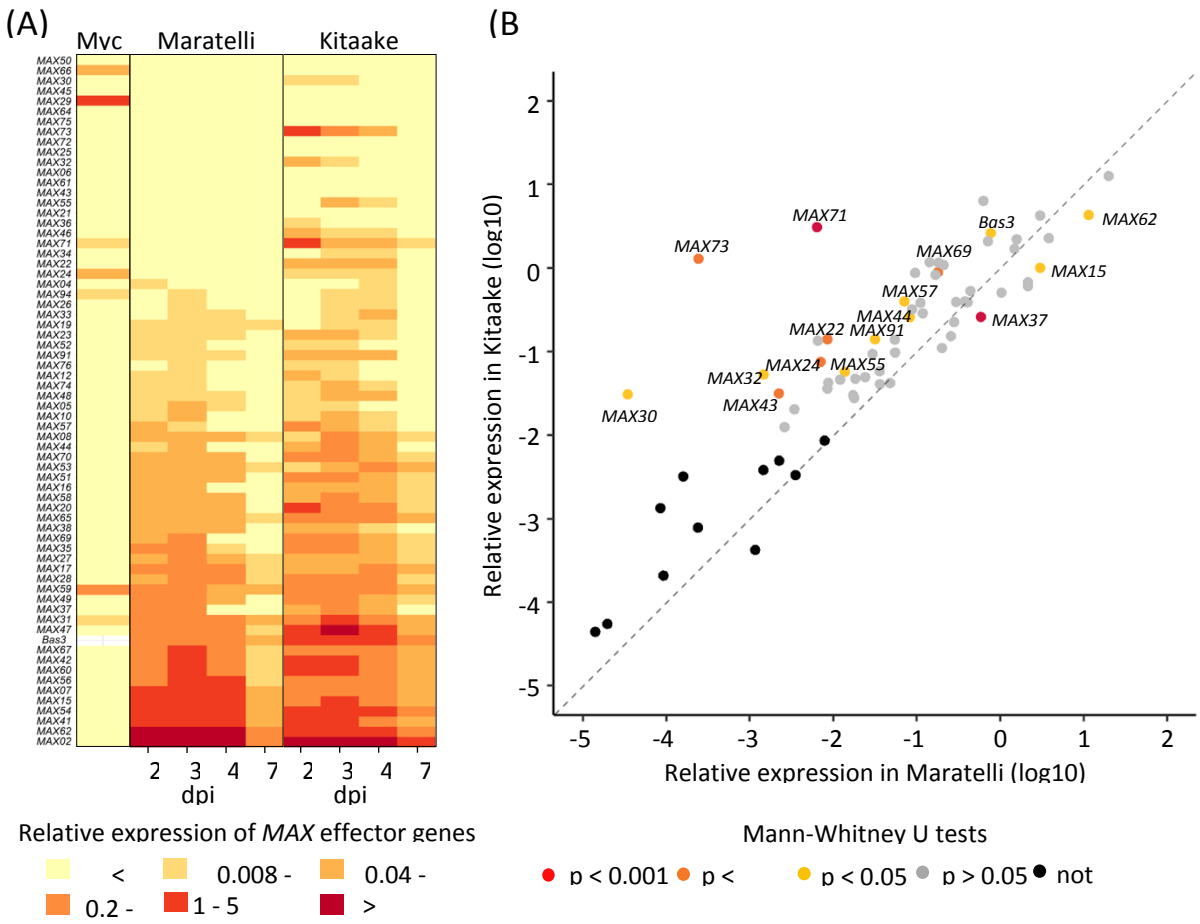


Figure 2. The expression of *MAX* genes is biotrophy-specific and is influenced by the host plant. (A) Transcript levels of *MAX* genes and the biotrophy marker gene *Bas3* were determined by qRT-PCR in the mycelium (Myc) of the *P. oryzae* isolate Guy11 grown for 5 days in liquid culture, and in infected leaves of the rice cultivars Maratelli and Kitaake at 2, 3, 4, and 7 days post inoculation (dpi) with Guy11. Relative expression levels were calculated using the constitutively expressed *MoEF1α* (*Elongation Factor 1α*) gene as a reference. The heatmap shows the median relative expression value for each gene (in log2 scale), calculated from 6 independent biological samples for the Myc condition, and 3 independent inoculation experiments (each with 5 independent leaf samples per time point) for each rice cultivar. Effectors were ranked from top to bottom by increasing relative expression values in Maratelli. Relative expression values were assigned to six categories: not expressed (<0.008), very weakly (0.008-0.04), weakly (0.04-0.2), moderately (0.2-1), strongly (1-5) and very strongly expressed (>5). (B) Scatter plot comparing the relative expression levels of MAX genes in Guy11-infected Maratelli and Kitaake cultivars. Each point shows the maximum median relative expression value (in log10 scale) calculated in the infection kinetics described in (A). Difference in effector relative expression levels between the two conditions was assessed by Mann-Whitney U tests and dots were colored according to significance results: grey ($p$>0.05), yellow ($p$<0.05), orange ($p$<0.001), red ($p$<0.0001), black (effectors not expressed in both conditions).

211 *Variability of the MAX effector repertoire.*

212 To investigate the genetic diversity of MAX effectors in *P. oryzae*, we analyzed their nucleotide diversity
213 per base pair ($\pi$), their ratio of non-synonymous to synonymous nucleotide diversity ($\pi_N/\pi_S$), and their
214 presence-absence polymorphism. Compared to other secreted proteins or other genes, MAX effector
215 orthogroups had higher $\pi$, and $\pi_N/\pi_S$ values, and lower presence frequency (S3 Figure). Orthogroups
216 including known avirulence genes like *AVR1-CO39*, *AvrPiz-t* and *AVR-Pik* featured among the most
217 diverse orthogroups of MAX effectors (S1 Data).

218 We categorized genes in the pangenome according to their presence frequencies [38], with core
219 genes present in all isolates, softcore genes present in >99% isolates, cloud genes present in 1-99% isolates
220 and shell genes present in <1% isolates. The majority of MAX effector genes were classified as cloud
221 (64/80 [80%] orthogroups), while the majority of other secreted proteins or other genes were classified as
222 core or softcore (1650/3283 [50.2%] and 6714/11404 [58.9%] orthogroups, respectively) (Figure 3A). Only
223 a minority of genes were present in multiple copies (MAX: 15/80 [18.8%]; other effectors: 746/3283
224 [22.7%]; other genes: 1439/11404 [12.6%]; Figure 3A). Assessment of the openness of the pan-genome by
225 iteratively subsampling isolates revealed a closed pangenome with a limited number of pan and core
226 genes for MAX effectors, other secreted proteins and the remainder of the gene space (Figure 3B).
227 Nucleotide diversity differed significantly between categories of the pangenome for non-MAX effectors
228 (Kruskal-Wallis test: H=181.17, d.f.=2, $p$<0.001) and other genes (Kruskal-Wallis test: H=225.25, d.f.=2,
229 $p$<0.001), but not for MAX effectors (Kruskal-Wallis test: H=2.50, d.f.=2, $p$>0.05). For non-MAX effectors
230 and other genes, nucleotide diversity $\pi$ was significantly higher in the cloud genes than in softcore genes
231 and core genes (Post-hoc Mann-Whitney U-tests, p<0.001; Figure 3C).

232 Together, these analyses show that the MAX effector repertoire is highly plastic compared to
233 other gene categories, both in terms of the presence/absence of orthogroups and the sequence variability
234 within orthogroups.

235

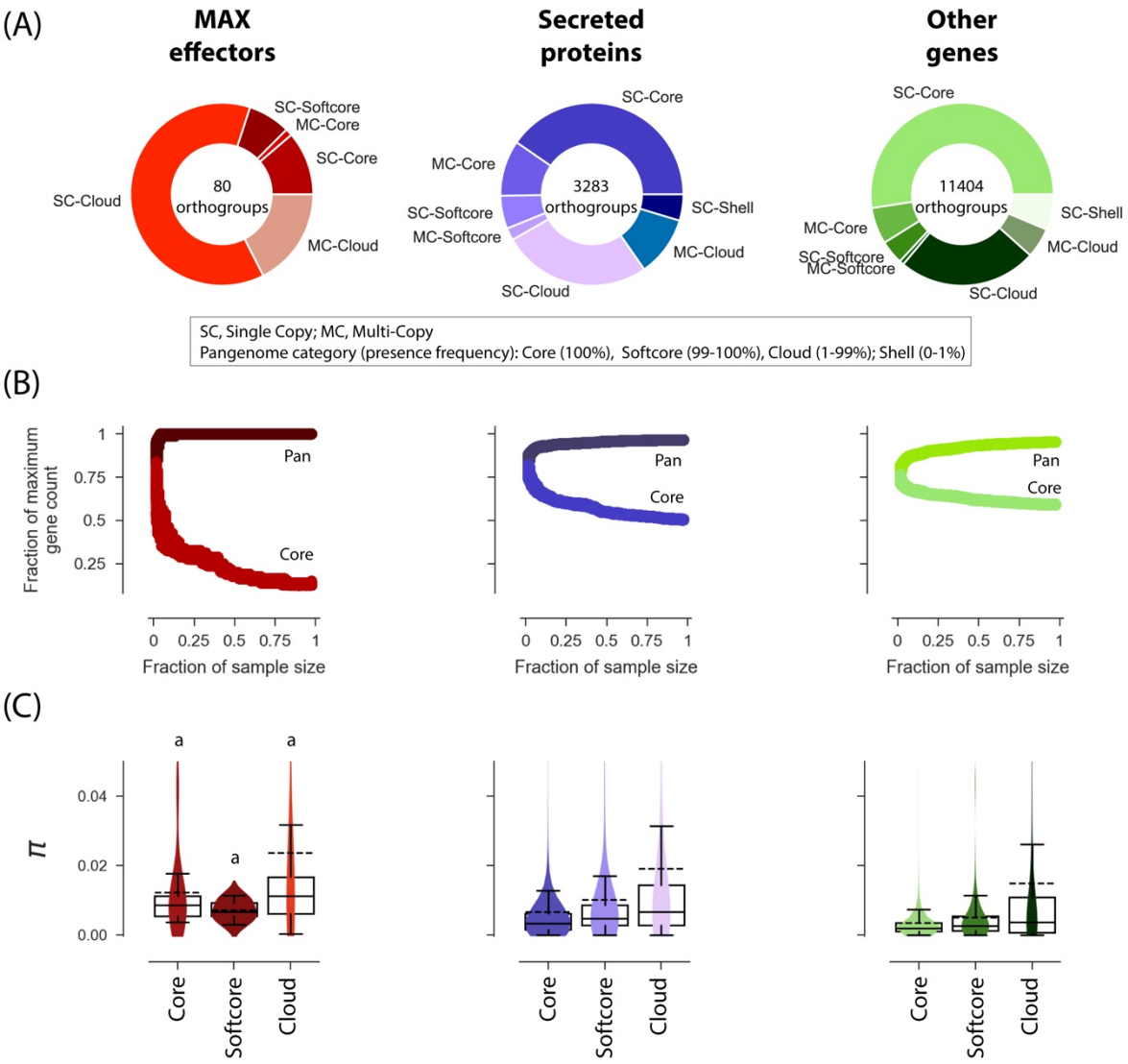


Figure 3. The pan-genome of *P. oryzae*. (A) Composition of the pangenome of MAX effectors, other secreted proteins, and other genes. (B) Rarefaction analysis of the size of pan- and core-genomes. For k ranging from two to the sample size minus one, pan- and core-genome sizes were computed for 1000 random combinations of k isolates. Subsample size is represented as a fraction of the sample size (n=121), and pan- and core-genome sizes as a fraction of maximum gene counts (reported at the center of donut plots in panel A). "core" genes are present in all isolates of a pseudo-sample of size k; "pan" qualifies genes that are not "core". (C) Nucleotide diversity per base pair ($\pi$) in core, softcore, and cloud genes. A number of data points were cropped from the nucleotide diversity plot for visually optimal presentation but included in statistical tests. In box plots, the dashed black line is the mean, the solid black line is the median. Shell genes were not included in the nucleotide diversity plot because it was not computable due to the small sample size or lack of sequence after filtering for missing data. Shared superscripts indicate non-significant differences (Post-hoc Mann-Whitney U-tests).

*Population subdivision.*

To investigate signatures of positive selection in the genome of *P. oryzae*, and identify candidate loci involved in host specificity, we first identified the divergent lineages represented in our dataset. We inferred population structure from 5.04e5 SNPs in single-copy core orthologs, using complementary approaches that make no assumption about random mating or linkage equilibrium. Both clustering analyses with the sNMF software [38] (Figure 4A) and neighbor-net phylogenetic networks [39] (Figure 4B) revealed consistent patterns that split genetic variation primarily by host of origin, with seven major lineages mainly associated with rice (*Oryza*), foxtail millet (*Setaria*), wheat (*Triticum*), ray-grass (*Lolium*), goosegrass (*Eleusine*), barnyard grass and maize (*Echinochloa* and *Zea*), and St. Augustine grass (*Stenotaphrum*).

Population subdivision inferred from MAX effectors using either 130 SNPs without missing data in single-copy core MAX effectors (Figure 4C) or presence/absence variation of all 80 MAX effector orthogroups (Figure 4D) revealed essentially the same groups as the analysis of the single-copy core orthologs. This indicates that genome-wide nucleotide variation, variation in MAX effector content, and nucleotide variation at MAX effectors reflected similar genealogical processes. The *Oryza* and *Setaria* lineages displayed exceptionally high presence/absence variation of MAX effectors (average Hamming distance between pairs of isolate: 0.123 and 0.095; Figure 4D), but only limited sequence variation at single copy core MAX effectors (average Hamming distance between pairs of isolate: 0.017 and 0.012; Mann-Whitney U-tests, $p<0.05$; Figure 4C).

Population subdivision was also apparent at the level of the global characteristics of genomes. Assembly size differed significantly among lineages (Kruskal-Wallis test: H=72.9, d.f.=4, p<0.0001), and genome assemblies for the *Oryza*-infecting lineage, in particular, were significantly shorter than assemblies from other groups (Post-hoc Mann-Whitney U-tests, p<0.001; S4 Figure). The number of predicted genes, which was positively and significantly correlated with assembly size (Spearman's $\rho=0.31$, $p<0.001$), also differed significantly among lineages and was the highest in the *Lolium*-infecting lineage and the lowest in the *Eleusine*-infecting lineage (Kruskal-Wallis test: H=19.4, d.f.=4, p<0.0001; S4 Figure). The distribution of the number of orthogroups in lineages was largely similar to the

275 distribution of the number of genes, with more orthogroups in the *Lolium*-infecting lineage and fewer in
276 the *Eleusine*-infecting lineage (S4 Figure).

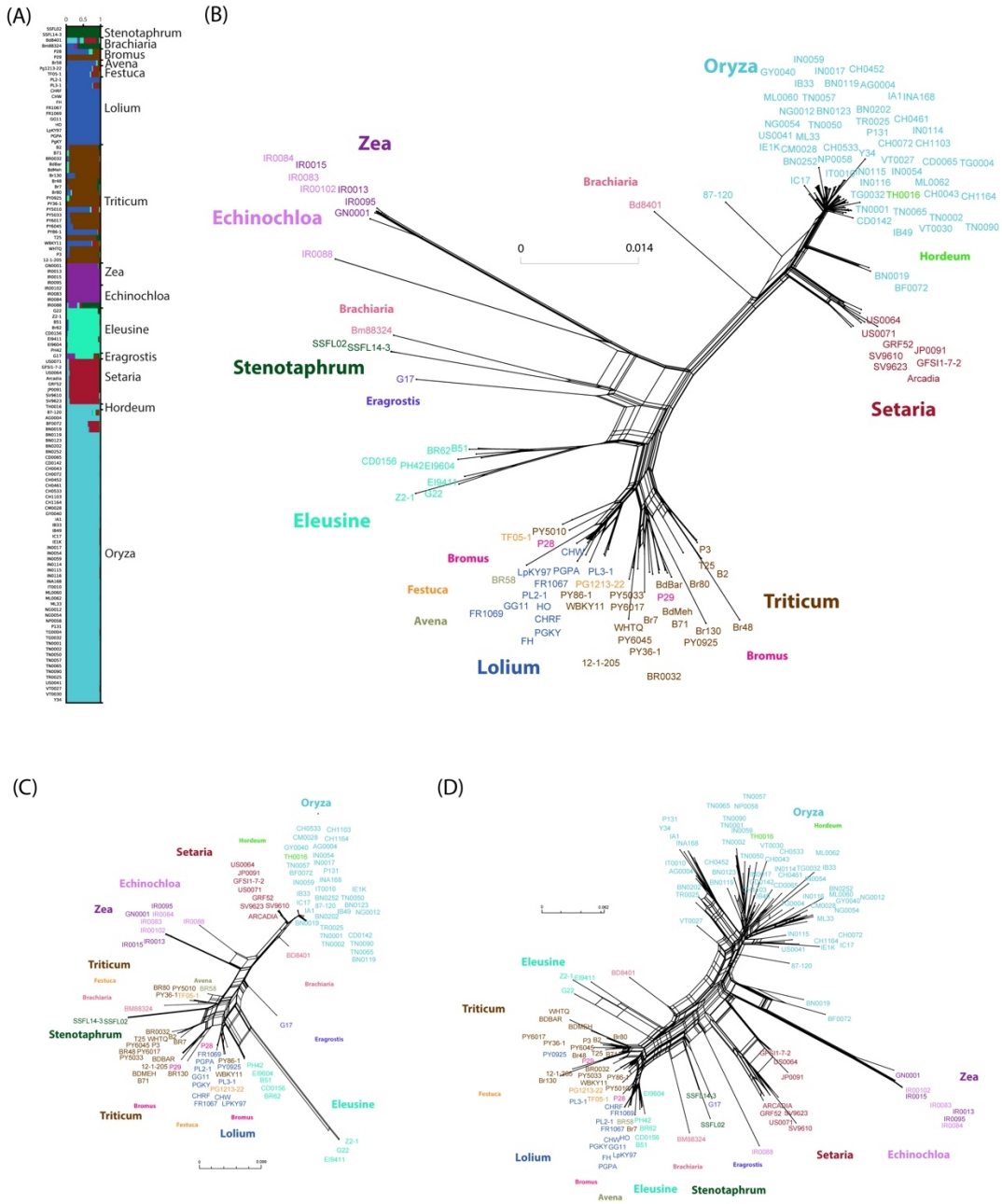


277

278 Figure 4. Population subdivision in 120 isolates of *Magnaporthe oryzae*. Population subdivision was inferred from (A-B) 5.04e5
279 single nucleotide polymorphisms (SNPs) without missing data identified in coding sequences of single-copy core orthologs, (C)
280 130 SNPs without missing data identified in coding sequences of single-copy core MAX effectors, (D) a table of presence/absence
281 data (coded as 0 and 1) for all 80 MAX effector orthogroups. (A) Genetic ancestry proportions for individual isolates in K=7
282 ancestral populations, as estimated using the sNMF clustering algorithm [38]; each isolate is depicted as a horizontal bar divided
283 into K segments representing the proportion of ancestry in K=7 inferred ancestral populations; host genus of origin is indicated
284 on the right side. (B-D) Neighbor-net phylogenetic networks estimated with SplitsTree [39], with isolate names colored

285 according to their host of origin. In (C), haplotypes repeated multiple times were represented by the first items in the following
286 lists: (BN0252, CD0065, CH0043, CH0072, CH0452, CH0461, IN0114, IN0115, IN0116), (IB33, ML0060, ML0062, ML33, NG0054,
287 NP0058, TG0004, TG0032, US0041, VT0027, VT0030), (TR0025, Y34), (CHRF, HO, LPKY97, P28).
288
289 *Loss of MAX effectors in specific lineages does not necessarily associate with host specificity.*
290 The comparison of the MAX effector content in the genomes of 120 *P. oryzae* isolates revealed extensive
291 presence/absence polymorphism between host-specific groups (S3 Table). To address the underlying
292 evolutionary mechanisms, we tested experimentally the hypothesis that MAX effector losses are
293 massively related to escape from receptor-mediated non-host resistance. Indeed, the loss of MAX
294 effectors in specific lineages of *P. oryzae* could primarily serve to escape from non-host resistance during
295 infections of novel plant species carrying immune receptors specifically recognizing these effectors. To
296 test this hypothesis, we focused on the *Oryza*- and *Setaria*-infecting lineages, as previous investigations
297 suggested that the *Oryza*-infecting lineage emerged by a host shift from *Setaria* and we found both groups
298 to be closely related (Figure 4) [21, 40]. Our strategy was to introduce into the *Oryza*-isolate Guy11 MAX
299 effectors absent from the *Oryza* lineage but present in the *Setaria* lineage, and to assess the ability of
300 these transgenic isolates to infect rice.
301 We identified three MAX orthogroups that were largely or completely absent from the *Oryza*
302 lineage, but present in the majority of isolates of the other lineages (S3 Table). Orthogroup MAX79
303 (OG0011591-1) was absent in all 52 *Oryza*-infecting isolates, while MAX83 (OG0011907), and MAX89
304 (OG0012141) were absent in 50 and 46 of them, respectively (S3 Table). Constructs carrying the genomic
305 sequence of *MAX79*, *MAX83* or *MAX89* derived from the *Setaria* isolate US0071 and under the control
306 of the strong infection specific promoter of the effector *AVR-Pia* were generated and stably introduced
307 into Guy11. For each construct, three independent transgenic lines were selected. Transgene insertion
308 was verified by PCR and the expression of transgenes was measured by qRT-PCR (S5 Figure). To test
309 whether the selected MAX effectors trigger immunity in rice, the transgenic isolates were spray-
310 inoculated onto a panel of 22 cultivars representative of the worldwide diversity of rice (S4 Table).
311 As controls, we used the MAX effectors *AVR-Pia*, which is rare outside the *Oryza* and *Setaria*
312 lineages, and *AVR1-CO39*, which is absent or pseudogenized in the *Oryza* lineage, but present in all other
313 host-specific lineages including *Setaria*. Both effectors are detected in rice by the paired NLR immune

receptors RGA4 and RGA5 from the *Pi-a/Pi-CO39* locus and thereby contribute, respectively, to host or non-host resistance in this plant species [41, 42].

As expected, isolates expressing *AVR1-CO39* or *AVR-Pia* triggered resistance in the rice variety Aichi Asahi that carries *Pi-a*, but caused disease on Nipponbare (*pi-a*$^{-}$) and other varieties lacking this *R* locus (Figure 5; S4 Table). Unlike the positive controls, the effectors MAX79, MAX83 and MAX89 were not recognized and did not induce resistance in any of the tested rice cultivars (Figure 5; S4 Table). The disease symptoms caused by the transgenic isolates carrying these effectors were similar to those observed for wild-type Guy11 or Guy11 isolates carrying an *RFP* (red fluorescent protein) construct. This suggests that these effectors do not significantly increase the virulence of Guy11.

These experiments show that despite their loss in the *Oryza*-infecting lineage of *P. oryzae,* and unlike AVR1-CO39, the effectors MAX79, MAX83, and MAX89 do not seem to induce non-host resistance in rice. Consequently, other mechanisms than escape from host immunity contributed to the loss of these MAX effectors during the putative host shift of *P. oryzae* from *Setaria* to *Oryza*.

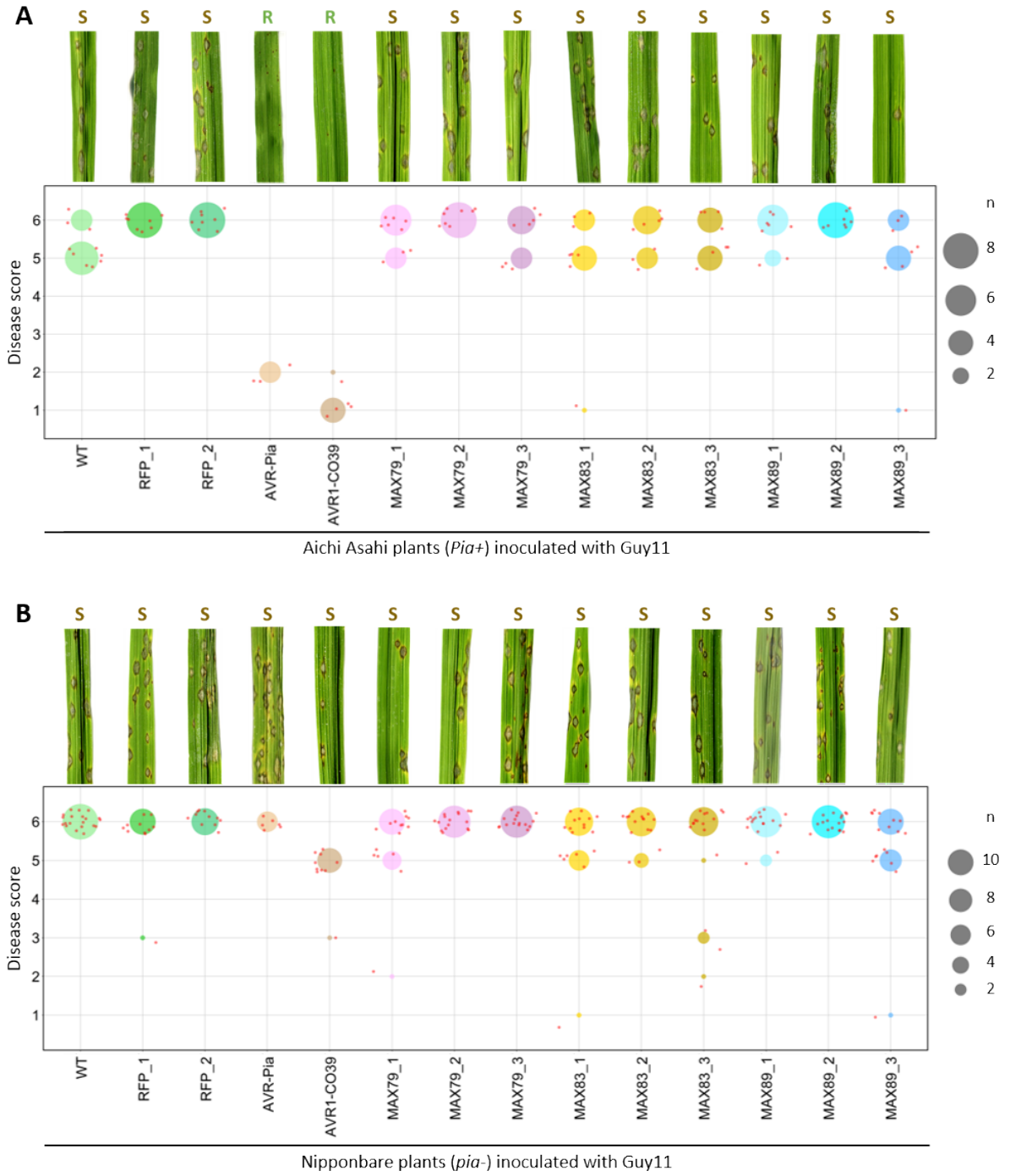


Figure 5. AVR1-CO39 contributes to non-host specificity in rice but not MAX79, MAX83 or MAX89. Wild type and transgenic isolates of *P. oryzae* Guy11 expressing the *RFP* (*red fluorescent protein*), *AVR-Pia, AVR1-CO39, MAX79*, *MAX83* or *MAX89* gene were spray-inoculated at 40 000 spores/ml on three-week-old rice plants of the cultivars Aichi Asahi (A) and Nipponbare (B). For each condition, representative disease phenotypes on rice leaves at seven days post-inoculation are shown (top panels, R: resistance, S: susceptibility). Disease phenotypes were also scored (from 1 [complete resistance] to 6 [high susceptibility]) on leaves from 3 to 5 individual rice plants and data are shown as dot plots (bottom panels). The size of each circle is proportional to the number of replicates (n) matching the corresponding score for each condition. Small red dots correspond to individual measurements. The experiment was performed twice for Aichi Asahi and four times for Nipponbare

for all isolates except for WT, AVR-Pia, and AVR1-CO39 control isolates. For these isolates, experiments were performed once on Aichi Asahi and twice on Nipponbare because disease phenotypes are well characterized in the literature.

*Signatures of balancing selection at MAX effectors.*

To investigate the impact of balancing selection on MAX effector evolution, we focused on single-copy core, softcore, and cloud orthogroups to avoid the possible effect of gene paralogy. We then computed $\pi$ (nucleotide diversity per bp), $F_{ST}$ (the amount of differentiation among lineages [43]), $\pi_N$ (non-synonymous nucleotide diversity), $\pi_S$ (synonymous nucleotide diversity), and $\pi_N/\pi_S$ (the ratio of non-synonymous to synonymous nucleotide diversity). Large values of $\pi$ and $\pi_N/\pi_S$, in particular, are possible indicators of a gene being under balancing selection.

Nucleotide diversity ($\pi$) differed significantly between groups of genes (Kruskal-Wallis test, H=509.9, d.f.=2, $p$ <0.001; Figure 6A; S5 Table). $\pi$ was significantly higher for the set of MAX effectors (average $\pi$: 0.0104, standard deviation: 0.0137), than for other secreted proteins (average $\pi$: 0.0079, standard deviation: 0.020), and other genes (average $\pi$: 0.0049, standard deviation: 0.014; Mann-Whitney U-tests, $p$<0.05), showing that MAX effectors, and to a smaller extent other secreted proteins, are more variable than a typical gene. At the lineage level, however, nucleotide diversity at MAX effectors tended to not significantly differ from other putative effectors, or other genes (S5 Table).

In addition to having greater nucleotide variation than other genes at the species level, MAX effectors also displayed a higher ratio of non-synonymous to synonymous nucleotide diversity (Figure 6B; S5 Table). The $\pi_N/\pi_S$ ratio differed significantly between groups of genes (Kruskal-Wallis tests $H$=101.4, $d.f.$=2, $p$<0.001), and the excess of non-synonymous diversity was significantly, and markedly, higher for MAX effectors (average $\pi_N/\pi_S$: 1.826, standard deviation: 3.847) than for other effectors (average $\pi_N/\pi_S$: 0.461, standard deviation: 1.600), and other genes (average $\pi_N/\pi_S$: 0.448, standard deviation: 1.463; Mann-Whitney U-tests, $p$<0.05). The higher $\pi_N/\pi_S$ of MAX effectors was mostly driven by differences in $\pi_N$ (Figure 6A; S5 Table). Twenty MAX effectors displayed values in the top 5% percentile of non-effector genes, far exceeding the four genes expected by chance ($p$<0.05). More specifically, 26 MAX effectors displayed $\pi_N/\pi_S$ values greater than 1, which is the value expected under neutrality. This included three well-known avirulence genes: *AVR1-CO39* ($\pi_N/\pi_S$=2.564), *AVR-Pik*

($\pi_N/\pi_S$=15.574), and *AvrPiz-t* ($\pi_N/\pi_S$=1.431). The average $\pi_N/\pi_S$ ratio was also higher at MAX effectors than other secreted proteins and other genes in all lineages, with significant differences in four lineages (Mann-Whitney U-tests, $p$<0.05), and the average $\pi_N/\pi_S$ was greater than one in the *Oryza* lineage (Figure 6B; S5 Table). Seven to eleven MAX effectors had $\pi_N/\pi s$>1 at the lineage level, representing 8% (*Setaria*-infecting lineage) to 41% (*Lolium*-infecting lineage) of MAX effectors with a defined $\pi_N/\pi s$ ratio (*Zea*/*Echinochloa* lineage excluded, as only three MAX effectors had a defined $\pi_N/\pi s$; S2 Data).

$\pi_N/\pi_S$>1 is a strong indication of multiallelic balancing selection (*i.e.*, multiple alleles at multiple sites are balanced), as single sites under very strong balancing selection cannot contribute enough non-synonymous variability to push the $\pi_N/\pi_S$ ratio above one [44]. To assess whether the adaptation of lineages to their respective hosts may contribute to the species-wide excess of non-synonymous diversity detected at MAX effectors, we estimated population differentiation. The differentiation statistic $F_{ST}$ differed significantly between groups of genes (Kruskal-Wallis tests $H$=8.731, *d.f.*=2, $p$=0.013), and differentiation was significantly higher for MAX effectors than for other secreted proteins and other genes (Figure 6A; S5 Table). $F_{ST}$ was also significantly, albeit relatively weakly, correlated with $\pi_N/\pi_S$ at MAX effectors (Spearman's $\rho$: 0.304, $p$=0.007; S6 Figure). These observations indicate that between-lineages differences in allele frequencies are greater for MAX effectors than for other secreted proteins or other genes, which may result from divergent selection exerted by hosts.

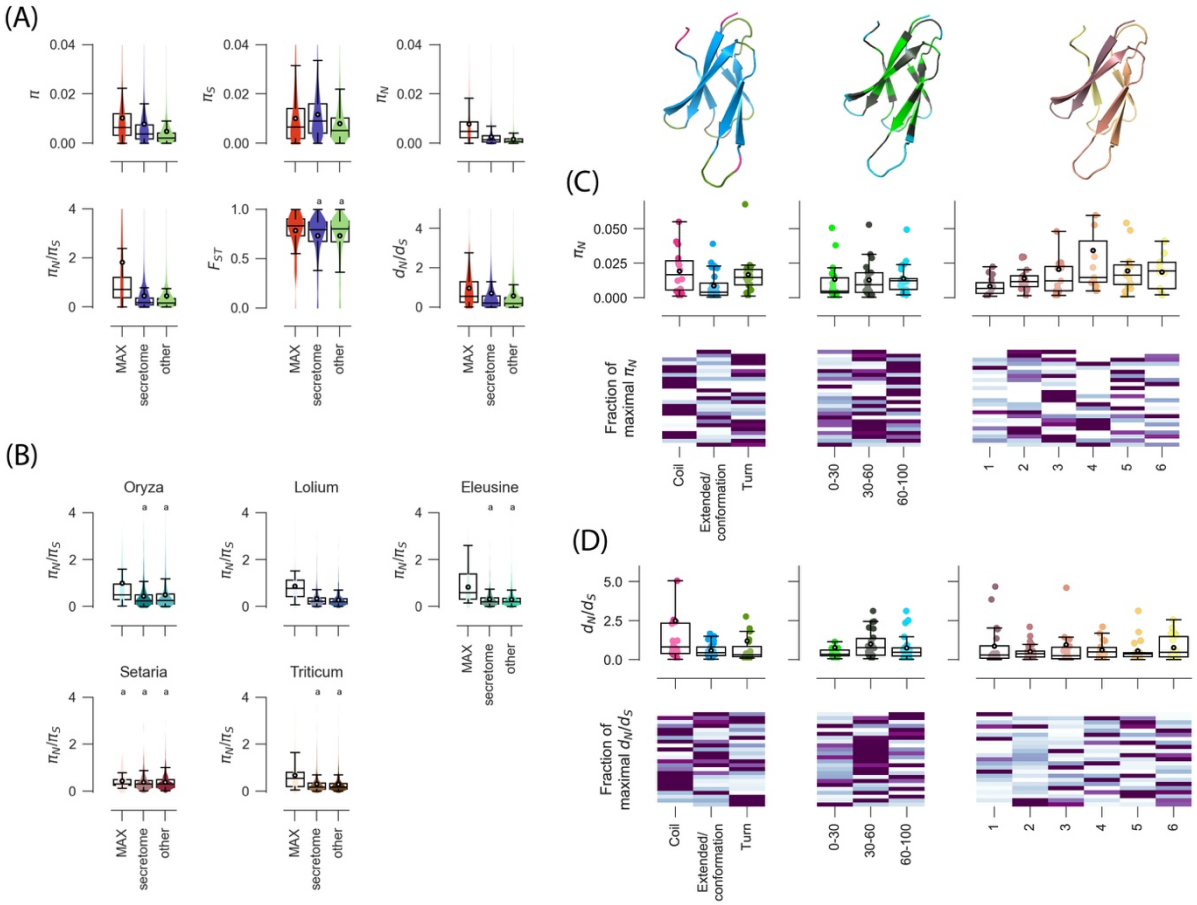


Figure 6. Summary statistics of polymorphism and divergence at MAX effectors, other secreted proteins (i.e., secretome), and other genes of *P. oryzae*. (A) Species-wide estimates of $\pi$ (nucleotide diversity per bp), $F_{ST}$ (the amount of differentiation among lineages), $\pi_N$ (non-synonymous nucleotide diversity per bp), $\pi_S$ (synonymous nucleotide diversity per bp), $\pi_N/\pi_S$ (the ratio of non-synonymous to synonymous nucleotide diversity), $d_N/d_S$ (the ratio of non-synonymous to synonymous rates of substitutions). (B) Lineage-specific estimates of $\pi_N/\pi_S$. (C) and (D) Species-wide estimates of $\pi_N$ and $d_N/d_S$ computed at MAX effectors with signatures of balancing selection ($\pi_N/\pi_S>1$; panel C) and signatures of directional selection ($d_N/d_S>1$; panel D) for different classes of secondary structure annotations highlighted on the three-dimensional structure of *AVR-Piz-t* above panel C: (i) structural features, with three subclasses: "extended conformation", "coils", and "turns"; (ii) solvent accessibility percentage of the Van der Waals surface of the amino acid sidechain, with three sub-classes: 0-30% (buried), 30-60% (intermediate), and 60-100% (exposed); (iii) structural domains, with six subclasses that grouped the coil, extended conformation and turn residues that define the six beta strands characteristic of MAX effectors. In the heatmaps, each line represents a MAX effector. For a given MAX effector and a given structural feature, the darkest color indicates the class of the secondary structure annotation for which the summary statistic is the highest. Only single-copy core, softcore, and cloud groups of orthologous genes were included in calculations. Shared superscripts indicate non-significant differences (post-hoc Mann-Whitney U-tests, $p>0.05$). A number of data points were cropped from plots in (A) and (B) for visually optimal presentation but included in statistical tests. In box plots, the black circle is the mean, the black line is the median.

*Signatures of recurrent directional selection at MAX effectors*

To detect adaptive molecular evolution, we collected orthologous sequences from outgroup *Pyricularia sp.* LS [45, 46] and estimated the $d_N/d_S$ ratio (the ratio of non-synonymous to synonymous substitution rates) using a maximum likelihood method [47]. Outgroup sequences could be retrieved for 10,174 out of 14,664 single-copy orthogroups, including 66 out of 94 single-copy orthologs of MAX effectors. The $d_N/d_S$ ratio differed significantly between groups of genes (Kruskal-Wallis tests $H$=45.812, $d.f.$=2, $p$<0.001; Figure 6A; S5 Table), and was higher for MAX effectors (average $d_N/d_S$: 0.977, s.d.: 1.316) than for other secreted proteins (average $d_N/d_S$: 0.711, s.d.: 1.722), and other genes (average $d_N/d_S$: 0.584, s.d.: 1.584; Mann-Whitney U-tests, $p$<0.05). The same pattern of higher $d_N/d_S$ for MAX effectors was observed at the lineage level (S5 Table). Twenty-four of the 66 MAX effectors with outgroup sequence (i.e., 36.4%) showed $d_N/d_S$>1 (S2 Data), which is a strong indication of directional selection. $d_N/d_S$>1 is only expected for genes that have experienced repeated bouts of directional selection which led to repeated fixations of amino-acid substitutions [44]. Eleven MAX effectors displayed signatures of both multiallelic balancing selection ($\pi_N/\pi_S$>1) and multiallelic directional selection ($d_N/d_S$>1).

The divergence data, therefore, indicate that a scenario of molecular co-evolution involving repeated selective sweeps may apply to a substantial fraction (at least one-third) of MAX effectors.

*Structural determinants of polymorphism and divergence at MAX effectors.*

Different parts of proteins can be under different selective forces. To investigate the relationships between the structural properties of MAX effectors and signatures of balancing or directional selection, we focused on MAX effectors with $d_N/d_S$ and $\pi_N/\pi_S$ ratios >1 and we computed $\pi_N$ and $d_N/d_S$ for different classes of secondary structure annotations, as computed by STRIDE from MAX effector structures predicted by homology modeling for each orthologous group [48] (S7 Figure). We used $\pi_N$ and not $\pi_N/\pi_S$ because the latter tended to be undefined due to relatively short sequence lengths. We defined three classes of secondary structure annotations: (1) structural features, with three subclasses: "extended conformation", "coils", and "turns"; (2) solvent accessibility percentage of the Van der Waals surface of the amino acid sidechain, with three sub-classes: 0-30% (buried), 30-60% (intermediate), and 60-100% (exposed); (3) structural domains, with six subclasses that grouped the coil, extended conformation and

turn residues that define the six beta strands characteristic of MAX effectors. We used the structure-guided alignment generated by TM-ALIGN to extract the secondary structure annotations of each amino acid of the MAX effector sequences (S7 Figure).

We found that $\pi_N$ significantly differed (Kruskal-Wallis tests $H$=8.504, $d.f.$=2, $p$=0.014) between subclasses of structural features (Figure 6C; S6 Table). In the 25 MAX effectors under multiallelic balancing selection that passed our filter on sequence length (at least ten sequences longer than 10bp, see Methods), $\pi_N$ was significantly higher at coils and turns, than at extended conformations (coils: $\pi_N$=0.0191; turns: $\pi_N$=0.0167; extended conformations: $\pi_N$=0.0086; posthoc Mann-Whitney U-tests, $p$<0.05), and 10 and 9 MAX effectors displayed their highest values of $\pi_N$ in coils and turns, respectively. $\pi_N$ did not significantly differ between relative solvent accessibility subclasses (Kruskal-Wallis tests $H$=2.308, $d.f.$=2, $p$=0.315), but differences were marginally significant between structural domains (Kruskal-Wallis tests $H$=11.035, $d.f.$=5, $p$=0.051). The third, fourth and fifth beta strands displayed the highest levels of non-synonymous diversity ($\pi_N$=0.0341, $\pi_N$=0.0341, and $\pi_N$=0.0341, respectively), and 18 out of 25 MAX effectors displayed their highest values of $\pi_N$ at one of these three beta strands (S6 Table).

In the 23 MAX effectors under multiallelic directional selection that passed our filter on sequence length (at least ten sequences longer than 10bp, see Methods), differences in $d_N/d_S$ were most pronounced between subclasses of structural features (Kruskal-Wallis tests $H$=5.499, $d.f.$=2, $p$=0.064), with higher average $d_N/d_S$ values for coils and turns ($d_N/d_S$=2.490 and $d_N/d_S$=1.184, respectively) than extended conformations ($d_N/d_S$=0.573) (Figure 6D; S6 Table). The average $d_N/d_S$ was also close to one for the 30-60% subclass of relative solvent accessibility ($d_N/d_S$=0.994), and 12 MAX effectors with signatures of directional selection had their highest $d_N/d_S$ values for this subclass, although differences were not significant.

Overall, these analyses show that multiallelic balancing and directional selection acted preferentially on coils and turns, but that the impact of two forms of selection on structural domains and solvent accessibility subclasses differs.

## DISCUSSION

*MAX effectors as model systems to investigate effector evolution.*

Effectors involved in coevolutionary interactions with host-derived molecules are expected to undergo non-neutral evolution. Yet, the role of natural selection in shaping polymorphism and divergence at effectors has remained largely elusive [2]. Despite the prediction of large and molecularly diversified repertoires of effector genes in many fungal genomes, attempts to probe into the evolutionary drivers of effector diversification in plant pathogenic fungi have been hindered by the fact that, until recently, no large effector families had been identified. In this study, we overcome the methodological and conceptual barrier imposed by effector hyper-diversity by building on our previous discovery [17] of an important, structurally-similar, but sequence-diverse family of fungal effectors called MAX. We used a combination of structural modeling, evolutionary analyses, and molecular plant pathology experiments to provide a comprehensive overview of polymorphism, divergence, gene expression, and presence/absence at MAX effectors. When analyzed species-wide or at the level of sub-specific lineages, ratios of non-synonymous to synonymous nucleotide diversity, as well as ratios of non-synonymous to synonymous substitutions, were consistently higher at MAX effectors than at other loci. At the species level, the two ratios were also significantly higher than expected under the standard neutral model for a large fraction of MAX effectors. The signatures of adaptive evolution detected at MAX effectors, combined with their extensive presence/absence variation, are consistent with their central role in coevolutionary interactions with host-derived ligands that impose strong selection on virulence effectors.

*Adaptive evolution at MAX effectors*

Rates of evolution determined from orthologous comparisons with outgroup sequences revealed that, for a large fraction of MAX effectors, non-synonymous changes have accumulated faster than synonymous changes. The fast rate of amino-acid change at MAX effectors is consistent with a classic arms race scenario, which entails a series of selective sweeps as new virulent haplotypes - capable of avoiding recognition by plant immune receptors that previously prevented pathogen multiplication - spread to high frequency [49, 50]. Furthermore, it is important to note that although large values of the $d_N/d_S$ ratio provide strong evidence for directional selection, small values do not necessarily indicate the lack thereof, as $d_N/d_S$ ratios represent the integration of genetic drift, constraint, and adaptive evolution [50][51]. Much

of the adaptive changes at MAX effectors probably took place before the radiation of *P. oryzae* on its various hosts. However, the observation that $d_N/d_S$ values determined from orthologous comparisons with outgroup are higher at the species level than at the sub-specific lineage level indicates that part of the signal of directional selection derives from inter-lineage amino acid differences associated with host-specialization. Our structural modeling indicates that it is preferentially "turns" and "coils", but also residues with intermediate solvent accessibility, which often evolve at an unusually fast rate, and therefore that these are probably the residues of MAX proteins preferentially involved in coevolutionary interactions with host-derived molecules.

MAX effectors are characterized by a remarkable excess of non-synonymous polymorphism, compared to synonymous polymorphism, at the species level, but also - albeit to a lesser extent - at the sub-specific lineage level. This raises the question of how polymorphisms are maintained in the face of adaptive evolution, given that selective sweeps under a classic arms race scenario are expected to erase variation [6, 9]. Directional selection restricted to host-specific lineages - i.e., local adaptation - may contribute to the signature of multiallelic balancing selection observed at the species level. The observation of a positive correlation between $\pi_N/\pi_S$ and the differentiation statistic $F_{ST}$, together with the fact that most MAX effectors are monomorphic at the lineage level, are consistent with a role of divergent selection exerted by hosts in the maintenance of species-wide diversity at MAX effectors. However, the finding that MAX effectors with a defined $\pi_N/\pi_S$ at the sub-specific lineage level (i.e., MAX effectors with $\pi_S \neq 0$) present a higher ratio than the other genes also indicates that the adaptive evolution process is not simply one of successive selective sweeps. This is consistent with balancing selection acting at the lineage level, through which polymorphisms in MAX virulence effectors are maintained due to spatiotemporal variation in selection pressures posed by the hosts – a process known as the trench-warfare model [49]. Our structural modeling suggests in particular that the "coils" and "turns" are the preferred substrate of these coevolutionary interactions leading to the maintenance of elevated polymorphism at MAX virulence effectors.

*Expression kinetics of MAX effectors*

Expression profiling showed that the MAX effector repertoire was induced specifically and massively during infection. Depending on the host genotype, between 64 and 78% of the MAX effectors were expressed and expression was particularly strong during the early stages of infection. These findings are consistent with previous studies that analyzed genome-wide gene expression during rice infection or specifically addressed MAX effector expression, and they reinforce the hypothesis that MAX effectors are crucial for fungal virulence and specifically involved in the biotrophic phase of infection [17, 52].

How this coordinated deployment of the MAX effectors is regulated remains largely unknown. Genome organization does not seem to be a major factor, since MAX effectors do not colocalize and more generally, there is no clustering of effectors in the *P oryzae* genome, only a slight enrichment in subtelomeric regions [52, 53]. This differs from other pathogenic fungi, such as *Leptosphaeria maculans*, for which early-expressed effectors are clustered in AT-rich isochores, and co-regulated by epigenetic mechanisms [54]. Analysis of promoter regions of MAX effectors did not identify common DNA motifs that may be targeted by transcription factors, and no such transcriptional regulators that would directly regulate large fractions of the effector complement of *P. oryzae* have been identified yet. The few known transcriptional networks controlled by regulators of *P. oryzae* pathogenicity generally comprise different classes of fungal virulence genes such as secondary metabolism genes or carbohydrate-active enzymes; they are not restricted to effectors or enriched in MAX effectors. For instance, Rgs1, a regulator of G-protein signaling necessary for appressorium development, represses the expression of 60 temporally co-regulated effectors in axenic culture and during the pre-penetration stage of plant infection [55]. However, among them are only two MAX effectors, *MAX15* (*MGG05424*) and *MAX67* (*MGG16175*). This suggests that multiple complementary mechanisms contribute to the precise coordination of MAX effector expression during rice invasion.

Expression profiling also revealed that the plant host genotype strongly influenced the expression of the MAX effector repertoire, suggesting that plasticity in effector expression may contribute to the adaptation of *P. oryzae* to its hosts. MAX effectors were stronger expressed in the more resistant Kitaake rice variety than in highly susceptible Maratelli rice. This is reminiscent of other pathogenic fungi, such as *Fusarium graminearum* and *L. maculans,* for which a relationship between host resistance levels and

543 effector expression was established [56, 57]. Specific experiments will have to be performed to analyze
544 in more detail this potential link between plant resistance and MAX effector expression.
545
546 *Presence/absence polymorphism of MAX effectors*
547 Pangenome analyses demonstrated extensive variability in the MAX effector repertoire. In cases where
548 MAX effectors are specifically absent from some lineages, but present in most or all others, it is tempting
549 to hypothesize that they experienced immune-escape loss-of-function mutations that directly contributed
550 to host range expansion or host shifts. A possible example of such a mechanism is the non-MAX effector
551 *PWT3* of *P. oryzae* that is specifically absent from the *Triticum*-infecting lineage [29]. PWT3 triggers
552 resistance in wheat cultivars possessing the *RWT3* resistance gene [58], and its loss was shown to
553 coincide with the widespread deployment of *RWT3* wheat. Similarly, the loss of the effector *AVR1-CO39*
554 (*MAX86*), which is specifically absent from the *Oryza*-infecting lineage and that is detected by the rice
555 NLR immune receptor complex RGA4/RGA5, has been suggested to have contributed to the initial
556 colonization of rice by the *Setaria*-infecting lineage [20, 31, 59]. Two other orthologous *P. oryzae*
557 effectors, *PWL1* and *PWL2*, exclude Eleusine and rice-associated isolates from infecting *Eragrostis*
558 *curvula*, and can, therefore, also be considered as host-specificity determinants [28, 60]. Interestingly,
559 ALPHAFOLD predicts PWL2 to adopt a MAX effector fold [61]. In our study, however, gene knock-in
560 experiments with *MAX79*, *MAX83,* and *MAX89* - specifically absent from the *Oryza*-infecting lineage -
561 did not reveal a strong effect on virulence towards a large panel of rice varieties. Hence, unlike AVR1-
562 CO39, these effectors are not key determinants of host-specificity. This suggests that overcoming non-
563 host resistance is not the only and maybe not the main evolutionary scenario behind the specific loss of
564 MAX effectors in the *Oryza*-infecting lineage. A possible alternative mechanism that can explain massive
565 MAX effector loss during host shifts is a lack of functionality in the novel host. Some MAX effectors
566 from a given lineage may have no function in the novel host, simply because their molecular targets are
567 absent or too divergent in the novel host. Cellular targets of fungal effectors remain unknown for the
568 most part, but knowledge of the molecular interactors of MAX effectors may help shed light on the drivers
569 of their presence/absence polymorphism.
570

*Concluding remarks*

The discovery of large, structurally-similar, effector families in pathogenic fungi and the increasing availability of high-quality whole genome assemblies and high-confidence annotation tools, pave the way for in-depth investigations of the evolution of fungal effectors by interdisciplinary approaches combining state-of-the-art population genomics, protein structure analysis, and functional approaches. Our study on MAX effectors in the model fungus and infamous cereal killer *P. oryzae* demonstrates the power of such an approach. Our investigations reveal the fundamental role of directional and balancing selection in shaping the diversity of MAX effector genes and pinpoint specific positions in the proteins that are targeted by these evolutionary forces. This type of knowledge is still very limited on plant pathogens, and there are very few studies compared to the plethoric literature on the evolution of virulence factors in human pathogens. Moreover, by revealing the concerted and plastic deployment of the MAX effector repertoire, our study highlights the current lack of knowledge on the regulation of these processes. A major challenge will now be to identify the regulators, target proteins and mode of action of MAX effectors, in order to achieve a detailed understanding of the relationships between the structure, function and evolution of these proteins.

## METHODS

### *Genome assemblies, gene prediction, and pan-genome analyses*

Among the 120 genome assemblies included in our study, 66 were already publicly available, and 54 were newly assembled (S1 Table). For the 54 newly assembled genomes, reads were publicly available for 50 isolates, and four additional isolates were sequenced (available under BioProject PRJEB47684). For the four sequenced isolates, DNA was extracted using the same protocol as in ref. [62]. For the 54 newly generated assemblies, CUTADAPT [63] was used for trimming and removing low-quality reads, reads were assembled with ABYSS 2.2.3 [64] using eight different K-mer sizes, and we chose the assembly produced with the K-mer size that yielded the largest N50. For all 120 genome assemblies, genes were predicted by BRAKER 1 [65] using RNAseq data from ref. [21] and protein sequences of isolate 70-15 (Ensembl Fungi release 43). To complement predictions from BRAKER, we also predicted genes using AUGUSTUS 3.4.0 [56][3] with RNAseq data from ref. [21] , protein sequences of isolate 70-15 (Ensembl Fungi release 43), and *Magnaporthe grisea* as the training set. Gene predictions from BRAKER and AUGUSTUS were merged by removing the genes predicted by AUGUSTUS that overlapped with genes predicted by BRAKER. Repeated elements were masked with REPEATMASKER 4.1.0 (http://www.repeatmasker.org/). The quality of genome assembly and gene prediction was checked using BUSCO [32]. The homology relationships among predicted genes were identified using ORTHOFINDER v2.4.0 [36]. The size of pan- and core-genomes was estimated using rarefaction, by resampling combinations of one to 119 genomes, taking a maximum of 100 resamples by pseudo-sample size. Sequences for each orthogroup were aligned at the codon level (i.e., keeping sequences in coding reading frame) with TRANSLATORX [66], using MAFFT v7 [67] as the aligner and default parameters for GBLOCKS [68].

### *Identification of effectors sensu lato, and MAX effectors*

We predicted the secretome by running SIGNALP 4.1 [69], TARGET [70], and PHOBIUS [62] to identify signal peptides in the translated coding sequences of 12000 orthogroups. Only proteins predicted to be secreted by at least two methods were retained. Transmembrane domains were identified using TMHMM [71] and proteins with a transmembrane domain outside the 30 first amino acids were excluded from the

predicted secretome. Endoplasmic reticulum proteins were identified with PS-SCAN (https://ftp.expasy.org/databases/prosite/ps_scan/), and excluded.

To identify MAX effectors, we used the same approach as in the original study that described MAX effectors [17]. We first used PSI-BLAST [33] to search for homologs of known MAX effectors (AVR1-CO39, AVR-Pia, AvrPiz-t, AVR-PikD, and ToxB) in the predicted secretome. Significant PSI-BLAST hits (e-value < e-4) were aligned using a structural alignment procedure implemented in TM-ALIGN [35]. Three rounds of HMMER [34] searches were then carried out, each round consisting of alignment using TM-ALIGN, model building using HMMBUILD, and HMM search using HMMSEARCH (e-value < e-3). Only proteins with two expected, conserved Cysteines less than 33-48 amino acids apart were retained in the first two rounds of HMMER searches, as described in ref. [17].

Subsequent evolutionary analyses were conducted on three sets of orthogroups: MAX effectors, putative effectors, and other genes. The "MAX" group corresponded to 80 orthogroups for which at least 10% of sequences were identified as MAX effectors. The "secreted proteins" groups corresponded to 3283 orthogroups that were not included in the MAX group, and for which at least 10% of sequences were predicted to be secreted proteins. The last group included the remaining 11404 orthogroups.

For missing MAX effector sequences, we conducted an additional similarity search to correct for gene prediction errors. For a given MAX orthogroup and a given isolate, if a MAX effector was missing, we used BLAST-N to search for significant hits using the longest sequence of the orthogroup as the query sequence, and the isolate's genome assembly as the subject sequence (S3 Table). We also corrected annotation errors, such as the presence of very short (typically <50bp) or very long (typically >500bp) introns, missing terminal exons associated with premature stops, or frameshifts caused by indels. All these annotation errors were checked, and corrected manually if needed, using the RNAseq data used in gene prediction in the INTEGRATIVE GENOME VIEWER [72, 73]. We also found that some orthogroups included chimeric gene resulting from erroneous merging of two genes that were adjacent in assemblies. This was the case for orthogroups OG0000093 and OG0010985, and we used RNA-seq data in the INTEGRATIVE GENOME VIEWER to split the merged genic sequences and keep only the sequence that corresponded to a MAX effector.

For evolutionary analyses conducted on single-copy orthologs, the 11 orthogroups that included paralogous copies of MAX effectors were split into sets of orthologous sequences using genealogies inferred using RAxML v8 [37], yielding a total of 94 single-copy MAX orthologs, of which 90 orthologs passed our filters on length and sample size to be included in evolutionary analyses (see below). For each split orthogroup, sets of orthologous sequences were assigned a number that was added to the orthogroup's identifier as a suffix (for instance paralogous sequences of orthogroup OG0000244 were split into orthogroups OG0000244_1 and OG0000244_2). Sequences were re-aligned using TRANSLATORX (see above) after splitting orthogroups.

All genome assemblies, aligned coding sequences for all orthogroups and single-copy orthologs are available in Zenodo, doi: 10.5281/zenodo.7689273.

*Homology modeling of MAX effectors*

To check that orthogroups predicted to be MAX effectors had the typical 3D structure of MAX effectors with two beta sheets of three beta strands each, eight experimental structures with MAX-like folds were selected as 3D templates for homology modeling (PDB identifiers of the templates: 6R5J, 2MM0, 2MM2, 2MYW, 2LW6, 5A6W, 5Z1V, 5ZNG). For each of the 94 MAX orthologous groups, one representative protein was selected and homology models of this 1D query relative to each 3D template were built using MODELLER [74] with many alternative query-template threading alignments. The structural models generated using the alternative alignments were evaluated using a combination of different structural scores (DFIRE [75], GOAP [76], QMEAN [77]). Our homology modeling procedure will be described with more details in a manuscript currently in preparation. The best structural models for the 94 representative sequences of each group of MAX orthologs are available at https://pat.cbs.cnrs.fr/magmax/model/. The correspondence between MAX orthogroups identifiers used in homology modeling and MAX orthogroups identifiers resulting from gene prediction is given in S2 Table.

669 *Evolutionary analyses*

670 Lineage-level analyses were conducted on a dataset from which divergent or introgressed isolates were
671 removed (G17 from *Eragrostis*, Bm88324 & Bd8401 from *Setaria*, 87-120; BF0072 and BN0019 from
672 *Oryza*; IR0088 from *Echinochloa*), to limit the impact of population subdivision within lineages. The
673 *Stenotaphrum*-infecting lineage was not included in lineage-level analyses due to the small sample size.

674 Nucleotide diversity [78] and population differentiation [43] were estimated using EGGLIB v3
675 [79]. Sites with more than 30% missing data were excluded. Orthogroups with less than 10 sequences
676 (*nseff*<10, *nseff* being the average number of used samples among sites that passed the missing data filter)
677 or shorter than 30bp (*lseff*<30, *lseff* being the number of sites used for analysis after filtering out sites with
678 too many missing data) were excluded from computations. For analyses of polymorphism at secondary
679 structure annotations, the cutoff on *lseff* was set at 10bp.

680 For the computation of $d_N/d_S$ and quantification of adaptive evolution, we used isolate NI919 of
681 *Pyricularia* sp. LS [45, 46] as the outgroup (assembly GCA_004337975.1, European Nucleotide Archive).
682 Genes were predicted in the outgroup assembly using EXONERATE V2.2 CODING2GENOME [80]. For each
683 gene, the query sequence was a *P. oryzae* sequence randomly selected among sequences with the fewest
684 missing data. In parsing EXONERATE output, we selected the sequence with the highest score, with a
685 length greater than half the length of the query sequence.

686 The $d_N/d_S$ ratio was estimated using a maximum likelihood approach (runmode=-2, CodonFreq=2
687 in CODEML [81]), in pairwise comparisons of protein coding sequences (*i.e.*, without using a phylogeny).
688 For each $d_N/d_S$ we randomly selected 12 ingroup sequences and computed the average $d_N/d_S$ across the 12
689 ingroup/outgroup pairs.

690 Kruskal-Wallis tests were performed using the SCIPY.STATS.KRUSKAL library in PYTHON 3.7.
691 Posthoc Mann-Whitney U-tests were performed using the SCIKIT_POSTHOCS library in PYTHON 3.7, with
692 p-values adjusted using the Bonferroni-Holm method.

693

694 *Constructs for the transformation of fungal isolates*

695 PCR products used for cloning were generated using the Phusion High-Fidelity DNA Polymerase
696 (Thermo Fisher) and the primers listed in S7 Table. Details of the constructs are given in S8 Table. Briefly,

the pSC642 plasmid (derived from the pCB1004 vector), containing a cassette for the expression of a gene of interest under the control of the *AVR-Pia* promoter (*pAVR-Pia*) and the *Neurospora crassa β-tubulin* terminator (*t-tub*), was amplified by PCR with primers oML001 and oTK609 for the insertion of MAX genes listed in S9 Table. The MAX genes *Mo_US0071_000070* (*MAX79*), *Mo_US0071_046730* (*MAX89*) and *Mo_US0071_115900* (*MAX83*), amplified by PCR from genomic DNA of the *P. oryzae* isolate US0071, were inserted into this vector using the Gibson Assembly Cloning Kit (New England BioLabs). The final constructs were linearized using the KpnI restriction enzyme (Promega) before *P. oryzae* transformation.

*Plant and fungal growth conditions*

Rice plants (*Oryza sativa*) were grown in a glasshouse in a substrate of 31% coconut peat, 30% Baltic blond peat, 15% Baltic black peat, 10% perlite, 9% volcanic sand, and 5% clay, supplemented with 3.5 $g.L^{-1}$ of fertilizer (Basacote® High K 6M, NPK 13-5-18). Plants were grown under a 12h-light photoperiod with a day-time temperature of 27 °C, night-time temperature of 21 °C, and 70% humidity. For spore production, the wild-type and transgenic isolates of *P. oryzae* Guy11 were grown for 14 days at 25°C under a 12h-light photoperiod on rice flour agar medium (20 $g.L^{-1}$ rice seed flour, 2.5 $g.L^{-1}$ yeast extract, 1.5% agar, 500.000U penicillin g), supplemented with 240 $\mu g.ml^{-1}$ hygromycin for transgenic isolates. For mycelium production, plugs of mycelium of *P. oryzae* Guy11 were grown in liquid medium (10 $g.L^{-1}$ glucose, 3 $g.L^{-1}$ $KNO_3$, 2 $g.L^{-1}$ $KH_2PO_4$, 2,5 $g.L^{-1}$ yeast extract, 500 000U penicillin g) for 5 days at 25°C in the dark under agitation.

*Fungal transformation*

Protoplasts from the isolate Guy11 of *P. oryzae* were transformed by heat shock with 10µg of KpnI-linearized plasmids for the expression of MAX effectors or RFP as described previously [74]. After two rounds of antibiotic selection and isolation of monospores, transformed isolates were genotyped by Phire Plant Direct PCR (Thermo Scientific) using primers described in S7 Table. The Guy11 transgenic isolates expressing *AVR-Pia* and *AVR1-CO39* were previously generated [82, 83].

*Fungal growth and infection assays*

For the analysis of interaction phenotypes, leaves of three-week-old rice plants were spray-inoculated with conidial suspensions (40 000 conidia.ml$^{-1}$ in water with 0.5% gelatin). Plants were incubated for 16 hours in the dark at 25°C and 95% relative humidity, and then grown for six days in regular growth conditions. Seven days after inoculation, the youngest leaf that was fully expanded at the time of inoculation was collected and scanned (Scanner Epson Perfection V370) for further symptoms analyses. Phenotypes were qualitatively classified according to lesion types: no lesion or small brown spots (resistance), small lesions with a pronounced brown border and a small gray center (partial resistance), and larger lesions with a large gray center or dried leaves (susceptibility). For the analysis of gene expression, plants were spray-inoculated with conidial suspensions at 50 000 conidia.ml$^{-1}$ (in water with 0.5% gelatin), and leaves were collected three days after inoculation.

*RNA extraction and qRT-PCR analysis*

Total RNA extraction from rice leaves or Guy11 mycelium and reverse transcription were performed as described by ref. [84]. Briefly, frozen leaves and mycelium were mechanically ground. RNA was extracted using TRI-reagent® (Sigma-Aldrich) and chloroform separation. Denaturated RNA (5µg) was retrotranscribed and used for quantitative PCR using GoTaq qPCR Master Mix according to the manufacturer's instructions (Promega) at a dilution of 1/10 for mycelium and 1/7 for rice leaves. The primers used are described in S7 Table. Amplification was performed as described by ref. [84] using a LightCycler480 instrument (Roche), and data were extracted using the instrument software. To calculate *MAX* gene expressions, the $2^{-\Delta\Delta CT}$ method and primers measured efficiency were used. Gene expression levels are expressed relative to the expression of constitutive reference gene *MoEF1α*.

*Statistical analyses of phenotypic data*

For expression comparison between Kitaake and Maratelli infection, all analyses were performed using R (www.r-project.org). The entire kinetic experiment was repeated three times with five biological replicates for each time point. For each variety, gene, and experimental replicate, values corresponding to the day post-inoculation with the highest median expression were extracted for statistical analyses.

752 Expression data were not normally distributed so for each gene, differences between varieties were
753 evaluated using non-parametric Mann-Whitney U-tests.
754

755 ## SUPPLEMENTARY MATERIALS

756 S1 Table. Genomic assemblies with metadata.
757 S2 Table. Nomenclature of MAX effectors.
758 S3 Table. Presence/absence of MAX effector orthologs.
759 S4 Table. The expression of MAX79, MAX83 and MAX89 in Guy11 does not trigger recognition in a panel of rice
760 varieties.
761 S5 Table. Gene average of summary statistics of polymorphism, differentiation and divergence.
762 S6 Table. $\pi_N$ and $d_N/d_S$ in different classes of secondary structure annotations for MAX effectors with $\pi_N/\pi_S>1$ and
763 $d_N/d_S>1$, respectively.
764 S7 Table. Primers for cloning and expression analyses.
765 S8 Table. Vector constructs.
766 S9 Table. Sequences of the MAX effectors in the isolate US0071 that were used for the complementation of Guy11.
767

768 S1 Figure. Expression patterns of MAX effectors during rice infection.
769 S2 Figure. Differential expression levels of MAX effectors upon infection of two different rice cultivars.
770 S3 Figure. Nucleotide diversity ($\pi$), ratio of non-synonymous to synonymous nucleotide diversity ($\pi_N/\pi_S$),
771 orthogroup frequency for MAX effectors, other secreted proteins, and other genes.
772 S4 Figure. Assembly size, number of predicted genes, and number of orthogroups in lineages of *M. oryzae*.
773 S5 Figure. MAX79, MAX83 and MAX89 are expressed in the transgenic Guy11 isolates upon rice inoculation.
774 S6 Figure. $F_{ST}$ versus $\pi_N/\pi_S$ at MAX effectors
775 S7 Figure. Secondary structure annotations of MAX effectors aligned with TM-ALIGN.
776

777 S1 Data. Summary statistics per orthogroup.
778 S2 Data. Summary statistics per MAX effector ortholog, species wide, and per lineage.
779

# REFERENCES


1. Schulze-Lefert P, Panstruga R. A molecular evolutionary concept connecting nonhost resistance, pathogen host range, and pathogen speciation. Trends in Plant Science. 2011;16(3):117-25. doi: 10.1016/j.tplants.2011.01.001.
2. Sánchez-Vallet A, Fouché S, Fudal I, Hartmann FE, Soyer JL, Tellier A, et al. The genome biology of effector gene evolution in filamentous plant pathogens. Annual review of phytopathology. 2018;56:21-40.
3. Haldane JBS. Disease and evolution. Ricerca Scient 1949;19:68-76.
4. Flor HH. Inheritance of pathogenicity in Melampsora lini. Phytopathology. 1942;32:653-69.
5. Barrett JA. Frequency-dependent selection in plant-fungal interactions. Philosophical Transactions of the Royal Society of London B, Biological Sciences. 1988;319(1196):473-83.
6. Bergelson J, Kreitman M, Stahl EA, Tian D. Evolutionary dynamics of plant R-genes. Science. 2001;292(5525):2281-5.
7. Brown JKM. Chance and selection in the evolution of barley mildew. Trends in Microbiology. 1994;2(12):470-5. PubMed PMID: 29.
8. Brown JKM. Durable resistance of crops to disease: a Darwinian perspective. Annual review of phytopathology. 2015;53:513-39.
9. Stahl EA, Dwyer G, Mauricio R, Kreitman M, Bergelson J. Dynamics of disease resistance polymorphism at the Rpm1 locus of Arabidopsis. Nature. 1999;400(6745):667-71.
10. Gladieux P, van Oosterhout C, Fairhead S, Jouet A, Ortiz D, Ravel S, et al. Extensive immune receptor repertoire diversity in disease-resistant rice landraces. bioRxiv. 2022:2022-12.
11. Bakker EG, Toomajian C, Kreitman M, Bergelson J. A genome-wide survey of R gene polymorphisms in Arabidopsis. The Plant cell. 2006;18(8):1803-18.
12. Bakker EG, Traw MB, Toomajian C, Kreitman M, Bergelson J. Low levels of polymorphism in genes that control the activation of defense response in Arabidopsis thaliana. Genetics. 2008;178(4):2031-43.
13. Ebert D, Fields PD. Host–parasite co-evolution and its genomic signature. Nature Reviews Genetics. 2020;21(12):754-68.
14. Ebbole DJ, Chen M, Zhong Z, Farmer N, Zheng W, Han Y, et al. Evolution and Regulation of a Large Effector Family of Pyricularia oryzae. Molecular Plant-Microbe Interactions. 2021;34(3):255-69.
15. Seong K, Krasileva KV. Computational structural genomics unravels common folds and novel families in the secretome of fungal phytopathogen Magnaporthe oryzae. Molecular Plant-Microbe Interactions. 2021;34(11):1267-80.
16. Seong K, Krasileva KV. Prediction of effector protein structures from fungal phytopathogens enables evolutionary analyses. Nature Microbiology. 2023;8(1):174-87.
17. de Guillen K, Ortiz-Vallejo D, Gracy J, Fournier E, Kroj T, Padilla A. Structure analysis uncovers a highly diverse but structurally conserved effector family in phytopathogenic fungi. PLoS Pathog. 2015;11(10):e1005228.
18. Savary S, Willocquet L, Pethybridge SJ, Esker P, McRoberts N, Nelson A. The global burden of pathogens and pests on major food crops. Nature ecology & evolution. 2019;3(3):430.
19. Fernandez J, Orth K. Rise of a cereal killer: the biology of Magnaporthe oryzae biotrophic growth. Trends in microbiology. 2018;26(7):582-97.
20. Couch BC, Fudal I, Lebrun M-H, Tharreau D, Valent B, van Kim P, et al. Origins of Host-Specific Populations of the Blast Pathogen *Magnaporthe oryzae* in Crop Domestication With Subsequent Expansion of Pandemic Clones on Rice and Weeds of Rice. Genetics. 2005;170(2):613-30. PubMed PMID: 61.
21. Pordel A, Ravel S, Charriat F, Gladieux P, Cros-Arteil S, Milazzo J, et al. Tracing the origin and evolutionary history of Pyricularia oryzae infecting maize and barnyard grass. Phytopathology. 2021;111(1):128-36.
22. Kato H, Yamamoto M, Yamaguchi-Ozaki T, Kadouchi H, Iwamoto Y, Nakayashiki H, et al. Pathogenicity, mating ability and DNA restriction fragment length polymorphisms of Pyricularia populations isolated from Gramineae, Bambusideae and Zingiberaceae plants. Journal of General Plant Pathology. 2000;66:30-47.
23. Urashima AS, Igarashi S, Kato H. Host range, mating type, and fertility of Pyricularia grisea from wheat in Brazil. Plant Disease. 1993;77(12):1211-6.
24. Igarashi S. Pyricularia em trigo. 1. Ocorrencia de Pyricularia sp noestado do Parana. Fitopatol Bras. 1986;11:351-2.
25. Milazzo J, Pordel A, Ravel S, Tharreau D. First scientific report of Pyricularia oryzae causing gray leaf spot disease on perennial ryegrass (Lolium perenne) in France. Plant Disease. 2019;103(5):1024-.
26. Islam MT, Croll D, Gladieux P, Soanes DM, Persoons A, Bhattacharjee P, et al. Emergence of wheat blast in Bangladesh was caused by a South American lineage of Magnaporthe oryzae. BMC biology. 2016;14(1):84.
27. Gladieux P, Condon B, Ravel S, Soanes D, Maciel JLN, Nhani A, et al. Gene Flow between Divergent Cereal- and Grass-Specific Lineages of the Rice Blast Fungus Magnaporthe oryzae. mBio. 2018;9(1).
28. Sweigard JA, Carroll AM, Kang S, Farrall L, Chumley FG, Valent B. Identification, Cloning, and Characterization of *PWL2*, a Gene for Host Species Specificity in the Rice Blast Fungus. The Plant cell. 1995;7(8):1221-33. PubMed PMID: 260.

29. Inoue Y, Vy TTP, Yoshida K, Asano H, Mitsuoka C, Asuke S, et al. Evolution of the wheat blast fungus through functional losses in a host specificity determinant. Science. 2017;357(6346):80-3.
30. Asuke S, Tanaka M, Hyon G-S, Inoue Y, Vy TTP, Niwamoto D, et al. Evolution of an Eleusine-specific subgroup of Pyricularia oryzae through a gain of an avirulence gene. Molecular Plant-Microbe Interactions. 2020;33(2):153-65.
31. Zheng Y, Zheng W, Lin F, Zhang Y, Yi Y, Wang B, et al. AVR1-CO39 is a predominant locus governing the broad avirulence of Magnaporthe oryzae 2539 on cultivated rice (Oryza sativa L.). Molecular plant-microbe interactions. 2011;24(1):13-7.
32. Simão FA, Waterhouse RM, Ioannidis P, Kriventseva EV, Zdobnov EM. BUSCO: assessing genome assembly and annotation completeness with single-copy orthologs. Bioinformatics. 2015;31(19):3210-2.
33. Altschul SF, Madden TL, Schäffer AA, Zhang J, Zhang Z, Miller W, et al. Gapped BLAST and PSI-BLAST: a new generation of protein database search programs. Nucleic acids research. 1997;25(17):3389-402.
34. Finn RD, Clements J, Eddy SR. HMMER web server: interactive sequence similarity searching. Nucleic acids research. 2011;39(suppl_2):29-37.
35. Zhang Y, Skolnick J. TM-align: a protein structure alignment algorithm based on the TM-score. Nucleic acids research. 2005;33(7):2302-9.
36. Emms DM, Kelly S. OrthoFinder: solving fundamental biases in whole genome comparisons dramatically improves orthogroup inference accuracy. Genome biology. 2015;16(1):157.
37. Stamatakis A. RAxML version 8: a tool for phylogenetic analysis and post-analysis of large phylogenies. Bioinformatics. 2014;30(9):1312-3.
38. Frichot E, Mathieu F, Trouillon T, Bouchard G, François O. Fast and efficient estimation of individual ancestry coefficients. Genetics. 2014;196(4):973-83.
39. Huson DH, Bryant D. Application of Phylogenetic Networks in Evolutionary Studies. Molecular Biology and Evolution. 2006;23(2):254-67.
40. Tosa Y, Osue J, Eto Y, Oh H-S, Nakayashiki H, Mayama S, et al. Evolution of an avirulence gene, AVR1-CO39, concomitant with the evolution and differentiation of Magnaporthe oryzae. Molecular Plant-Microbe Interactions. 2005;18(11):1148-60.
41. Cesari S, Thilliez G, Ribot C, Chalvon V, Michel C, Jauneau A, et al. The rice resistance protein pair RGA4/RGA5 recognizes the Magnaporthe oryzae effectors AVR-Pia and AVR1-CO39 by direct binding. The Plant cell. 2013;25(4):1463-81. Epub 2013/04/04. doi: 10.1105/tpc.112.107201. PubMed PMID: 23548743; PubMed Central PMCID: PMCPMC3663280.
42. Okuyama Y, Kanzaki H, Abe A, Yoshida K, Tamiru M, Saitoh H, et al. A multifaceted genomics approach allows the isolation of the rice Pia-blast resistance gene consisting of two adjacent NBS-LRR protein genes. The Plant Journal. 2011;66(3):467-79.
43. Weir BS, Cockerham CC. Estimating F-statistics for the analysis of population structure. Evolution. 1984;38:1358-70. PubMed PMID: 283.
44. Hahn MW. Molecular population genetics: Oxford University Press; 2018.
45. Hirata K, Kusaba M, Chuma I, Osue J, Nakayashiki H, Mayama S, et al. Speciation in Pyricularia inferred from multilocus phylogenetic analysis. Mycological Research. 2007;111(7):799-808.
46. Gómez Luciano LB, Tsai IJ, Chuma I, Tosa Y, Chen Y-H, Li J-Y, et al. Blast fungal genomes show frequent chromosomal changes, gene gains and losses, and effector gene turnover. Molecular Biology and Evolution. 2019;36(6):1148-61.
47. Yang Z. Likelihood ratio tests for detecting positive selection and application to primate lysozyme evolution. Molecular biology and evolution. 1998;15(5):568-73.
48. Frishman D, Argos P. Knowledge-based protein secondary structure assignment. Proteins: Structure, Function, and Bioinformatics. 1995;23(4):566-79.
49. Clay K, Kover PX. The Red Queen hypothesis and plant/pathogen interactions. Annual review of Phytopathology. 1996;34(1):29-50.
50. Van Valen L. A new evolutionary law. 1973.
51. Yang Z, Bielawski JP. Statistical methods for detecting molecular adaptation. Trends in ecology & evolution. 2000;15(12):496-503.
52. Yan X, Tang B, Ryder LS, MacLean D, Were VM, Eseola AB, et al. The transcriptional landscape of plant infection by the rice blast fungus Magnaporthe oryzae reveals distinct families of temporally co-regulated and structurally conserved effectors. bioRxiv. 2022:2022-07.
53. Chiapello H, Mallet L, Guerin C, Aguileta G, Amselem J, Kroj T, et al. Deciphering Genome Content and Evolutionary Relationships of Isolates from the Fungus Magnaporthe oryzae Attacking Different Host Plants. Genome Biol Evol. 2015;7(10):2896-912. Epub 2015/10/11. doi: 10.1093/gbe/evv187. PubMed PMID: 26454013; PubMed Central PMCID: PMCPMC4684704.
54. Soyer JL, El Ghalid M, Glaser N, Ollivier B, Linglin J, Grandaubert J, et al. Epigenetic control of effector gene expression in the plant pathogenic fungus Leptosphaeria maculans. PLoS genetics. 2014;10(3):e1004227.

55. Tang B, Yan X, Ryder LS, Cruz-Mireles N, Soanes DM, Molinari C, et al. Rgs1 is a regulator of effector gene expression during plant infection by the rice blast fungus Magnaporthe oryzae. bioRxiv. 2022:2022-09.
56. Fall LA, Salazar MM, Drnevich J, Holmes JR, Tseng M-C, Kolb FL, et al. Field pathogenomics of Fusarium head blight reveals pathogen transcriptome differences due to host resistance. Mycologia. 2019;111(4):563-73.
57. Sonah H, Zhang X, Deshmukh RK, Borhan MH, Fernando WGD, Belanger RR. Comparative transcriptomic analysis of virulence factors in Leptosphaeria maculans during compatible and incompatible interactions with canola. Frontiers in plant science. 2016;7:1784.
58. Arora S, Steed A, Goddard R, Gaurav K, O'Hara T, Schoen A, et al. A wheat kinase and immune receptor form host-specificity barriers against the blast fungus. Nature Plants. 2023:1-8.
59. Farman ML, Eto Y, Nakao T, Tosa Y, Nakayashiki H, Mayama S, et al. Analysis of the structure of the *AVR1-Co39* avirulence locus in virulent rice-infecting isolates of *Magnaporthe grisea*. Molecular Plant-Microbe Interactions. 2002;15:6-16. PubMed PMID: 90.
60. Kang S, Sweigard Ja Fau - Valent B, Valent B. The PWL host specificity gene family in the blast fungus Magnaporthe grisea. Molecular Plant Microbe Interactions. 1995;(0894-0282 (Print)).
61. Brabham HJ, Gómez De La Cruz D, Were V, Shimizu M, Saitoh H, Hernández-Pinzón I, et al. Barley MLA3 recognizes the host-specificity determinant PWL2 from rice blast (M. oryzae). bioRxiv. 2022:2022-10.
62. Thierry M, Charriat F, Milazzo J, Adreit H, Ravel S, Cros-Arteil S, et al. Maintenance of divergent lineages of the Rice Blast Fungus Pyricularia oryzae through niche separation, loss of sex and post-mating genetic incompatibilities. PLoS pathogens. 2022;18(7):e1010687.
63. Martin M. Cutadapt removes adapter sequences from high-throughput sequencing reads. EMBnet journal. 2011;17(1):10-2.
64. Simpson JT, Wong K, Jackman SD, Schein JE, Jones SJM, Birol I. ABySS: a parallel assembler for short read sequence data. Genome research. 2009;19(6):1117-23.
65. Hoff KJ, Lange S, Lomsadze A, Borodovsky M, Stanke M. BRAKER1: unsupervised RNA-Seq-based genome annotation with GeneMark-ET and AUGUSTUS. Bioinformatics. 2015;32(5):767-9.
66. Abascal F, Zardoya R, Telford MJ. TranslatorX: multiple alignment of nucleotide sequences guided by amino acid translations. Nucleic acids research. 2010;38(suppl_2):W7-W13.
67. Katoh K, Toh H. Recent developments in the MAFFT multiple sequence alignment program. Briefings in Bioinformatics. 2008;9(4):286-98. doi: 10.1093/bib/bbn013. PubMed PMID: ISI:000256756400004.
68. Castresana J. Selection of conserved blocks from multiple alignments for their use in phylogenetic analysis. Molecular biology and evolution. 2000;17(4):540-52.
69. Petersen TN, Brunak S, Von Heijne G, Nielsen H. SignalP 4.0: discriminating signal peptides from transmembrane regions. Nature methods. 2011;8(10):785-6.
70. Emanuelsson O, Nielsen H, Brunak S, Von Heijne G. Predicting subcellular localization of proteins based on their N-terminal amino acid sequence. Journal of molecular biology. 2000;300(4):1005-16.
71. Krogh A, Larsson B, Von Heijne G, Sonnhammer ELL. Predicting transmembrane protein topology with a hidden Markov model: application to complete genomes. Journal of molecular biology. 2001;305(3):567-80.
72. Robinson JT, Thorvaldsdóttir H, Turner D, Mesirov JP. igv. js: an embeddable JavaScript implementation of the Integrative Genomics Viewer (IGV). Bioinformatics. 2023;39(1):btac830.
73. Robinson JT, Thorvaldsdóttir H, Winckler W, Guttman M, Lander ES, Getz G, et al. Integrative genomics viewer. Nature biotechnology. 2011;29(1):24-6.
74. Webb B, Sali A. Protein Structure Modeling with MODELLER. Methods Mol Biol. 2021;2199(1940-6029 (Electronic)):239–55.
75. Zhou H, Zhou Y. Distance-scaled, finite ideal-gas reference state improves structure-derived potentials of mean force for structure selection and stability prediction. Protein science. 2002;11(11):2714-26.
76. Zhou H, Skolnick J. GOAP: a generalized orientation-dependent, all-atom statistical potential for protein structure prediction. Biophysical journal. 2011;101(8):2043-52.
77. Benkert P, Tosatto SCE, Schomburg D. QMEAN: A comprehensive scoring function for model quality assessment. Proteins: Structure, Function, and Bioinformatics. 2008;71(1):261-77.
78. Tajima F. Evolutionary relationship of DNA sequences in finite populations. Genetics. 1983;105(2):437-60.
79. Siol M, Coudoux T, Ravel S, De Mita S. EggLib 3: A python package for population genetics and genomics. Molecular Ecology Resources. 2022;22(8):3176-87.
80. Slater GSC, Birney E. Automated generation of heuristics for biological sequence comparison. BMC bioinformatics. 2005;6(1):1-11.
81. Yang Z. PAML: a program package for phylogenetic analysis by maximum likelihood. Computer applications in the biosciences. 1997;13(5):555-6.
82. Ribot C, Césari S, Abidi I, Chalvon V, Bournaud C, Vallet J, et al. The M agnaporthe oryzae effector AVR 1–CO 39 is translocated into rice cells independently of a fungal-derived machinery. The Plant Journal. 2013;74(1):1-12.

958 83. Ortiz D, De Guillen K, Cesari S, Chalvon V, Gracy J, Padilla A, et al. Recognition of the Magnaporthe
959 oryzae effector AVR-Pia by the decoy domain of the rice NLR immune receptor RGA5. The Plant cell.
960 2017;29(1):156-68.
961 84. Pélissier R, Buendia L, Brousse A, Temple C, Ballini E, Fort F, et al. Plant neighbour-modulated
962 susceptibility to pathogens in intraspecific mixtures. Journal of experimental botany. 2021;72(18):6570-80.
963